Table 1 **Photographs of broad-collared, deep-sea (>1,500-m) enteropneusts**

Designation	Quality of photo	Depth (m)	Location
Enteropneust[1]	High	4,735	30° S 177° W
Organism[2]	Low	3,786	15° N 58° W
Organism[2]	Low	3,681	10° N 92° W
No designation[3]	Low	2,907	70° S 125° W
Enteropneust[4]	Low	2,018	31° S 114° E
Enteropneust[4]	Low	6,725	15° S 175° W
Lophenteropneust[5]	Low	8,259	6° S 152° E
Lophenteropneust[5]	Low	8,254	12° S 166° E
Lophenteropneust[6]	Medium	5,160	12° N 159° W
Enteropneust[7]	Medium	5,099	14° N 127° W
Enteropneust[8]	Low	2,040	21° S 167° E
Enteropneust (Fig. 3a)	High	1,670	46° S 174° E
Enteropneust (Fig. 3b)*	High	2,715	43° N 127° W
Enteropneust (Fig. 3c)	High	3,000	53° N 35° W
Enteropneust (Fig. 3d)†	High	3,036	19° N 156° W
Enteropneust (Fig. 3e)	High	2,355	53° N 35°W

The table describes previously published photographs and those in Fig. 3; it omits deep-living enteropneusts with collars approximately circular in cross-section (*Saxipendium coronatum*[16], *Glandiceps abyssicola*[22] and undescribed[23–25]).
*Six similar-looking enteropneusts were photographed on different dates at 36° N 123° W at depths between 3,200 and 3,498 m.
†A similar-looking enteropneust was photographed at 34° N 121° W at a depth of 1,960 m.

pharynx contained four acoel flatworms, evidently commensals, each about 1 mm long, and the post-hepatic intestine contained two intact harpacticoid copepods, possibly also commensals.

From an evolutionary point of view, our most significant finding is that the conspicuous width of the collar of *T. bullocki* is not due to the presence of tentacles. This species is therefore certainly not a lophenteropneust in the sense intended by Lemche[5]. This raises the question as to whether any of the enteropneusts visible in deep-sea photographs are actually lophenteropneusts. We therefore examined all of the photographic evidence, both published and unpublished (Fig. 3, Table 1). We found that photographs of low to moderate quality are inadequate to demonstrate the presence or absence of collar tentacles. Conversely, none of the high-resolution photographs with the potential to resolve collar tentacles ever showed such structures. Additionally, one observer in a submersible, who obtained a close view (but no photographs) of deep-sea enteropneusts, saw no tentacles[18]. In sum, there is no evidence that lophenteropneusts exist as originally described. They can be removed from the list of provocative evolutionary intermediates (although the evolutionary model they engendered—namely enteropneusts giving rise to pterobranchs—might still turn out to have merit on other grounds[14]). Although the lophenteropneust hypothesis resulted from a misinterpretation of low-resolution photographs, it has been a valuable stimulus for research on deep-sea hemichordates[19–21]. □

Received 24 November 2004; accepted 24 January 2005; doi:10.1038/nature03382.

1. Bourne, D. W. & Heezen, B. C. A wandering enteropneust from the abyssal Pacific, and the distribution of 'spiral' tracks on the sea floor. *Science* **150,** 60–63 (1965).
2. Ewing, M. & Davis, R. A. in *Deep Sea Photography* (ed. Hersey, J. B.) 259–294 (Johns Hopkins Press, Baltimore, Maryland, 1967).
3. Jacobs, S. S., Bruchhausen, P. M. & Bauer, E. B. *Hydrographic Stations, Bottom Photographs, Current Measurements, and Nephelometer Profiles. Eltanin Reports, Cruises 32–36* (Lamont-Doherty Geological Observatory, Palisades, New York, 1970).
4. Heezen, B. C. & Hollister, C. D. *The Face of the Deep* (Oxford Univ. Press, New York, 1971).
5. Lemche, H., Hansen, B., Madsen, F. J., Tendal, O. S. & Wolff, T. Hadal life as analyzed from photographs. *Vidensk. Meddr. Dansk Naturh. Foren.* **139,** 262–336 (1976).
6. Thiel, H. Structural aspects of the deep-sea benthos. *AMBIO Spec. Rep.* **6,** 25–31 (1979).
7. Foell, E. J. & Pawson, D. L. Photographs of invertebrate megafauna from abyssal depths of the north-eastern equatorial Pacific Ocean. *Ohio J. Sci.* **86,** 61–68 (1986).
8. Gaillard, C. Recent organism traces and ichnofacies on the deep-sea floor off New Caledonia, southwestern Pacific. *Palaios* **6,** 302–315 (1991).
9. Bateson, W. The ancestry of the Chordata. *Q. J. Microsc. Sci.* **26,** 535–571 (1886).
10. Jollie, M. The origin of chordates. *Acta Zool. Stockh.* **54,** 81–100 (1973).
11. Dilly, P. N. The pterobranch *Rhabdopleura compacta*: its nervous system and phylogenetic position. *Symp. Zool. Soc. Lond.* **36,** 1–16 (1975).
12. Jefferies, R. P. S. in *Major Events in Early Vertebrate Evolution* (ed. Ahlberg, P. E.) 40–66 (Taylor & Francis, London, 2001).
13. Lowe, C. J. *et al.* Anteroposterior patterning in hemichordates and the origin of the chordate nervous system. *Cell* **113,** 853–865 (2003).
14. Cameron, C. B., Garey, J. R. & Swalla, B. J. Evolution of the chordate body plan: new insights from phylogenetic analysis of deuterostome phyla. *Proc. Natl Acad. Sci. USA* **97,** 4469–4474 (2000).
15. Woodwick, K. H. in *Taxonomic Atlas of the Benthic Fauna of the Santa Maria Basin and the Western Santa Barbara Channel* Vol. 14 (eds Blake, J. A., Scott, P. H. & Lissner, A.) 251–259 (Santa Barbara Museum of Natural History, Santa Barbara, 1993).
16. Woodwick, K. H. & Sensenbaugh, T. *Saxipendium coronatum*, new genus, new species (Hemichordata: Enteropneusta): the unusual spaghetti worms of the Galápagos Rift hydrothermal vents. *Proc. Biol. Soc. Wash.* **98,** 351–365 (1985).
17. Young, C. M. in *Ecosystems of the Deep Oceans* (ed. Tyler, P. A.) 381–426 (Elsevier, Amsterdam, 2003).
18. Pawson, D. Deep-sea dreams: diary of a mad lophenteropneust watcher. *Deep-Sea Newsl.* **32,** 6–7 (2003).
19. Tendal, O. S. What became of Lemche's lophenteropneust? *Deep-Sea Newsl.* **27,** 21–24 (1998).
20. Tendal, O. S. Lemche's lophenteropneust widely known but still an enigma. *Deep-Sea Newsl.* **28,** 8 (1999).
21. Gage, J. D. & Tyler, P. A. *Deep Sea Biology, a Natural History of Organisms at the Deep-Ocean Floor* (Cambridge Univ. Press, Cambridge, 1991).
22. Spengel, J. W. *Fauna und Flora des Golfes von Neapel* Monograph 18, *Die Enteropneusten des Golfes von Neapel* (Friedländer, Berlin, 1893).
23. Menzies, R. J., George, R. Y. & Rowe, G. T. *Abyssal Environment and Ecology of the World Oceans* (Wiley, New York, 1973).
24. Thorndike, E. M., Gerard, R. D., Sullivan, L. G. & Paul, A. Z. in *The Ocean Floor* (eds Scrutton, R. A. & Talwani, M.) 255–275 (Wiley, Chichester, 1982).
25. Bett, B. J. UK Atlantic margin environmental survey: introduction and overview of bathyal benthic ecology. *Cont. Shelf Res.* **21,** 917–956 (2001).

Acknowledgements We thank C. B. Cameron and R. P. S. Jefferies for valuable taxonomic advice, and B. J. Bett, J. Barry, R. Logeman, B. H. Robison, R. J. Singleton, R. C. Vrijenhoek and the crews and pilots of the research vessels *Western Flyer*, *Akedemik Mstislav Keldysh* and *G.O. Sars*, the manned submersibles 'Mir1' and 'Mir2', and the ROVs 'Tiburon' and 'Bathysaurus' for animal collection, photography, and unpublished observations. This study was partly under the auspices of the MAR-ECO Project within the Census of Marine Life Program and was partly supported by the New Zealand Foundation for Research, Science and Technology.

Competing interests statement The authors declare that they have no competing financial interests.

Correspondence and requests for materials should be addressed to N.D.H. (nholland@ucsd.edu).

Ancient co-speciation of simian foamy viruses and primates

William M. Switzer[1], Marco Salemi[2], Vedapuri Shanmugam[1], Feng Gao[3], Mian-er Cong[1], Carla Kuiken[4], Vinod Bhullar[1], Brigitte E. Beer[5], Dominique Vallet[6], Annie Gautier-Hion[6], Zena Tooze[7], Francois Villinger[8], Edward C. Holmes[9] & Walid Heneine[1]

[1]HIV and Retrovirology Branch, Division of HIV/AIDS Prevention, National Center for HIV, STD, and TB Prevention, Centers for Disease Control and Prevention, 1600 Clifton Road, MS G-19, Atlanta, Georgia 30333, USA
[2]Department of Pathology, Immunology and Laboratory Medicine, University of Florida, 1600 SW Archer Road, Gainesville, Florida 32610, USA
[3]Human Vaccine Institute, Duke University, 0112E Research Park III Durham, North Carolina 27710, USA
[4]Los Alamos National Laboratory, Los Alamos, New Mexico 87545, USA
[5]Southern Research Institute, 431 Aviation Way, Frederick, Maryland 21701, USA
[6]CNRS-Université Rennes I, Ethology, Evolution, Ecology, Station Biologique, 35380 Paimpont, France
[7]Cercopan, 4 Ishie Lane, c/o Housing Estate, PO Box 826, Calabar, Cross River State, Nigeria
[8]Department of Pathology, Winship Cancer Center, Emory University, 1365B Clifton Road, Atlanta, Georgia 30322, USA
[9]Department of Zoology, University of Oxford, South Parks Road, Oxford OXI 3PS, UK

Although parasite–host co-speciation is a long-held hypothesis, convincing evidence for long-term co-speciation remains elusive, largely because of small numbers of hosts and parasites studied and uncertainty over rates of evolutionary change[1–5]. Co-speciation is especially rare in RNA viruses, in which cross-species transfer is the dominant mode of evolution[6–9]. Simian foamy viruses (SFVs) are ubiquitous, non-pathogenic retroviruses that infect all primates[10,11]. Here we test the co-speciation

hypothesis in SFVs and their primate hosts by comparing the phylogenies of SFV polymerase and mitochondrial cytochrome oxidase subunit II from African and Asian monkeys and apes. The phylogenetic trees were remarkably congruent in both branching order and divergence times, strongly supporting co-speciation. Molecular clock calibrations revealed an extremely low rate of SFV evolution, 1.7×10^{-8} substitutions per site per year, making it the slowest-evolving RNA virus documented so far. These results indicate that SFVs might have co-speciated with Old World primates for at least 30 million years, making them the oldest known vertebrate RNA viruses.

Co-speciation of a host and its parasite is most likely if the parasite is transmitted vertically, causes a persistent infection and is present in a wide range of hosts[9]. Foamy viruses (FVs) are exogenous, persistent, and non-pathogenic retroviruses in the subfamily *Spumaretrovirinae* that have been isolated from a broad range of mammals, including horses, cows, cats and nonhuman primates (NHPs)[10,11].

We first inferred phylogenetic trees for the SFV polymerase gene (*pol*) from 44 different monkey and ape species originating from both Asia and Africa, and one New World monkey (Supplementary Information). The *pol* gene is highly conserved and is easily amplifiable from divergent SFVs[11]. To infer the host phylogeny, we used mitochondrial (mtDNA) cytochrome oxidase subunit II (COII) sequences from 55 primate species (Supplementary Information). COII has previously been shown to be a powerful marker of primate phylogeny[12–14].

As expected, phylogenetic analysis of the COII sequences produced a tree similar to the known taxonomic relationships of the primates, and to those estimated from other genes[12–19]. The COII tree was composed of four monophyletic lineages within the Hominoidea (*Pan*/*Homo*, *Gorilla*, *Pongo* and *Hylobates*) and seven monophyletic lineages within the Cercopithecoidea, infraorder Catarrhini (Colobidae, *Trachypithecus*/*Pygathrix*/*Colobus*, *Cercopithecus*/*Chlorocebus*/*Erythrocebus*, *Allenopithecus*, *Macaca*, *Mandrillus*/*Cercocebus* and *Papio*/*Theropithecus*/*Lophocebus*) with the tree rooted with the New World *Ateles* sequence (Fig. 1a). Remarkably, the SFV tree formed two major monophyletic groups consisting of Hominoidea and Cercopithecoidea taxa similar to the clustering order of the COII tree (Fig. 1b). In addition, within the Hominoidea and Cercopithecoidea SFV clades, branching orders similar to those in the COII tree were observed (Fig. 1b). Within the Cercopithecoidea, the *Trachypithecus* SFV sequence was the basal taxon with the formation of seven additional clades, comprising *Cercopithecus*/*Chlorocebus*/*Erythrocebus*/African *Macaca*, *Allenopithecus*, *Cercocebus*/*Mandrillus*, African *Colobus*, Asian *Macaca*, *Papio*/*Theropithecus* and *Lophocebus* taxa. The SFV sequence from *Ateles* was excluded from the phylogenetic analysis because it did not seem to be a reliable outgroup. Similar trees were obtained by using both maximum-likelihood and neighbour-joining methods (data not shown), illustrating the strength of the primate and SFV phylogenetic relationships.

In total, we found statistically significant support ($P = 0.007$) for 22 co-speciation events between the 44 SFV and 55 COII-species specific sequences. Comparison of the SFV and COII trees (Fig. 2) by using reconciliation analyses shows both the congruent Hominoidea and Cercopithecoidea host superfamilies and SFV lineages and the identical clustering of specific subfamilies, such

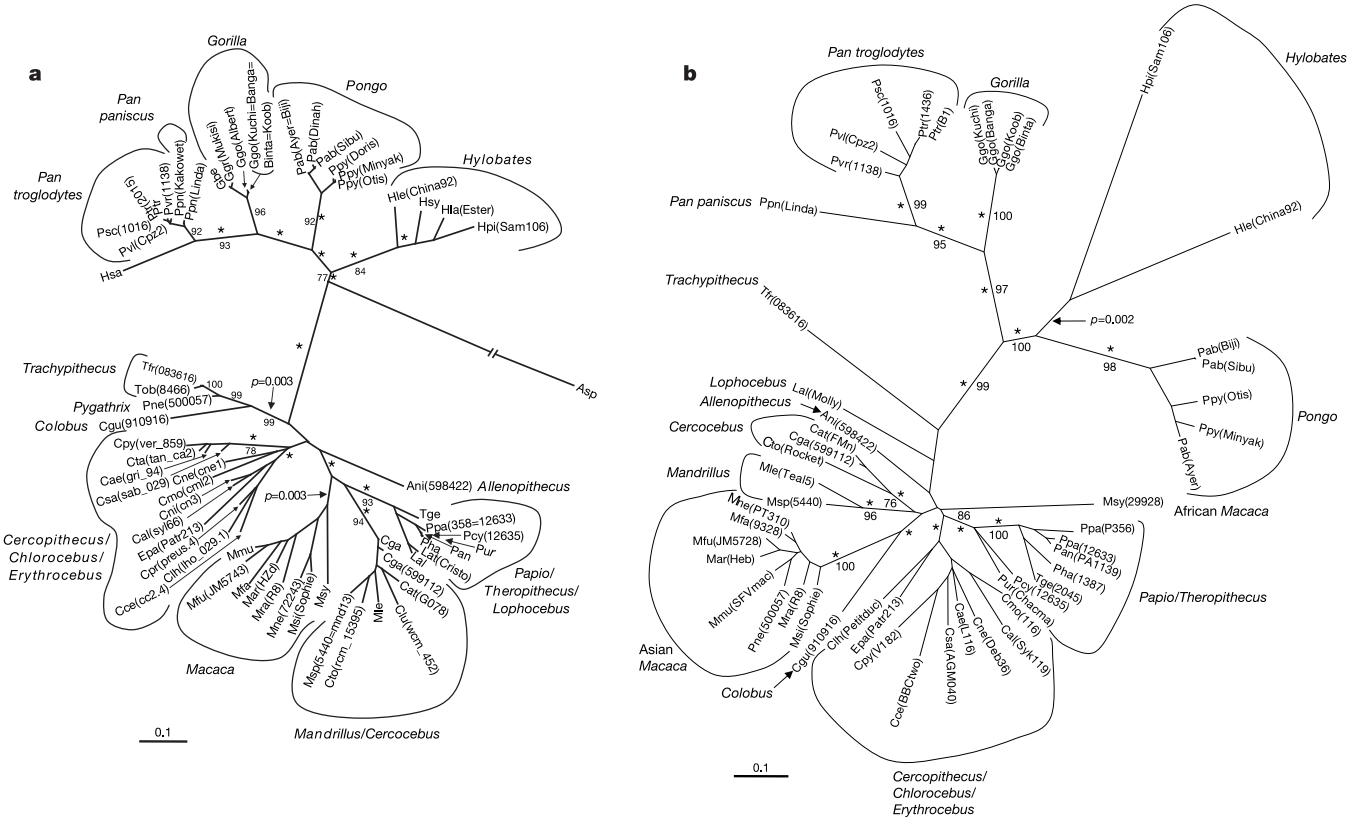

Figure 1 Congruence of host/parasite phylogenies. Phylogenetic relationships of (**a**) primate COII (500 base pairs) and (**b**) SFV *pol* sequences (425 base pairs) inferred by maximum-likelihood analysis. Support for the branching order was determined by 1,000 bootstrap replicates run on neighbour-joining trees using the maximum-likelihood substitution model and the zero branch length test (significance is indicated with *P* values on the branches; asterisks indicate $P < 0.001$). Only bootstrap values 70% or greater are shown. Branch lengths are drawn to scale except for the *Ateles* (Asp) COII sequence; the bar indicates 0.1 nucleotide substitutions per site. Primate taxon codes are provided in Supplementary Information.

as Homininae (*Gorilla* and *Pan*), Ponginae (*Pongo*) and Cercopithecinae (*Papio*). This is the first study to demonstrate such a comprehensive co-speciation relationship between exogenous viruses and their hosts.

Evidence for co-speciation of SFV and their primate hosts was also apparent on closer examination of sequences from individual primate species and subspecies within each clade (Fig. 1b). For example, SFV sequences from each of the Bornean (*Pongo pygmaeus*, Ppy) and Sumatran orangutans (*P. abelii*, Pab) formed well-supported sister taxa within the orangutan SFV lineage. However, one SFV sequence (PabAyer) from a Sumatran orangutan clustered with the Bornean SFVs (PpyOtis and PpyMinyak), indicating a possible interspecies transmission to this particular animal. Furthermore, SFV sequences from gibbons (*Hylobates*; HpiSam106 and HleChina92), gorillas (*Gorilla*; GgoBanga, GgoKuchi, GgoBinta and GgoKoob) and each chimpanzee species (*Pan paniscus* and *P. troglodytes*; PpnLinda and PtrB1, PvlCpz2, Psc1016, Pvr1138, respectively) and from each subspecies of common chimpanzee (*P. t. troglodytes* (PtrB1), *P. t. verus* (Pvr1138), *P. t. vellerosus* (PvlCpz2) and *P. t. schweinfurthii* (Psc1016)) formed separate branches in the respective monophyletic ape lineages.

Although there was strong phylogenetic support for a broad co-evolution of primates and SFV, some instances of cross-species infections were evident. In addition to the SFV from a Sumatran orangutan noted above, the SFV sequence from a Douc langur (*Pygathrix nemaeus*, Pne500057) clustered with those from macaques and the African colobus sequence (*Colobus guereza*, Cgu910916) clustered with those from Asian macaques in the SFV tree (bootstrap support less than 60%) (Fig. 1b) rather than with SFV from an Asian langur (*Trachypithecus francoisi*, Tfr083616). Because all three animals were not wild-born, it is likely that their atypical SFVs were acquired from other primate species during captivity. Therefore, despite long-standing co-speciation with SFV, some primates may remain susceptible to infection with variant SFV from different species. In contrast to the monophyly of the *Papio* and *Lophocephus* taxa in the COII tree, the *Lophocebus* SFV sequence (LalMolly) formed a weakly supported lineage separate from the *Papio* SFV indicative of another cross-species infection. However, when SFVs from additional *Lophocebus* taxa were included in the analysis, they clustered with *Papio* SFV as expected (data not shown)[16,19].

A significant match between host and parasite phylogenies might also be produced under cross-species transmission if viruses are more likely to jump between related host species[6–9]. To address this hypothesis we asked whether the divergence times of the COII and SFV trees are internally consistent. We found a strong linear relationship ($r = 0.8486$, $P < 0.0001$) between the branch lengths for the host and SFV gene trees, indicating that the accumulation of genetic diversity has occurred over an equivalent period in both data sets (Fig. 3). In addition, we found a strong agreement between the internode divergence times of the SFV and COII trees and the fossil record (Table 1). For example, we infer the separation of the chimpanzee and gorilla lineages to be 9.8–10.8 million years (Myr) ago with the SFV tree and 10.6–16.4 Myr ago with the COII tree, in general agreement with the divergence times of 7.4–8.8 Myr ago obtained by others[18,19]. In addition, the separation of the chimpanzee and human lineages in the COII tree is in excellent agreement with the fossil record estimate of about 5–6 Myr ago[18,19]. Given that SFV has a wide distribution among prosimian and simian primates, our data also imply that SFVs have coexisted in primates for an evolutionary history stretching at least 65 Myr. Furthermore, because divergent FVs asymptomatically infect other mammalian orders[10], the origin of FVs might even date back to the diversification of the placental mammals at more than 100 Myr

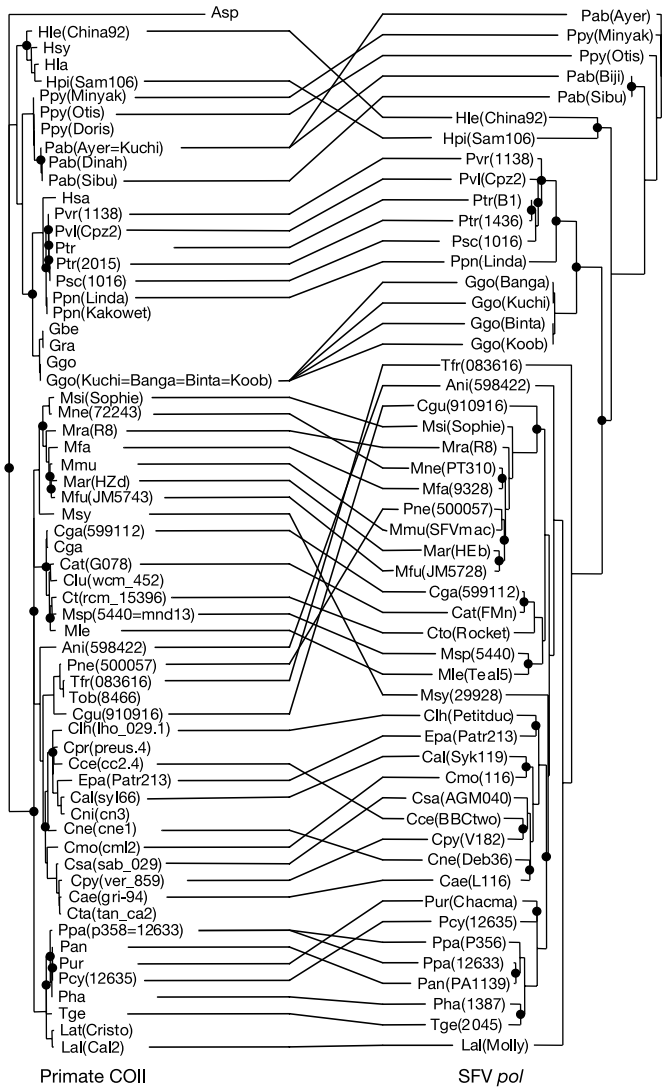

Figure 2 Co-evolutionary relationships of primate COII and SFV *pol* phylogenetic trees based on reconciliation analysis. Primate COII and SFV associations are indicated by connecting lines. Crossed lines indicate incongruent evolutionary host–virus relationships. SFV-infected hosts with identical COII sequences are indicated with multifurcated connecting lines. Hosts without SFV infection are indicated by the absence of a connecting line. Solid circles at nodes are inferred co-speciation events. The 22 co-speciation events were significantly higher than expected by chance in randomizations of both trees ($P = 0.007$).

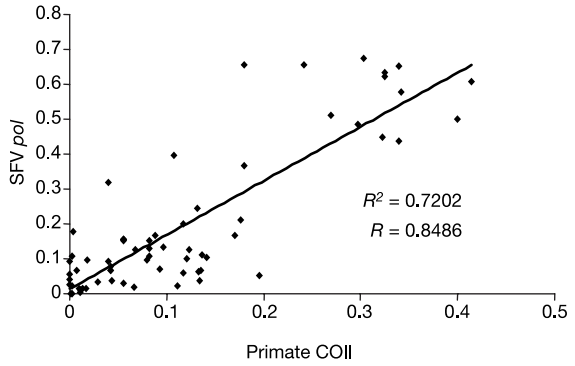

Figure 3 Correlation of branch lengths (substitutions per site) of primate COII and SFV *pol* phylogenetic trees. A statistically significant correlation ($P < 0.0001$) of the branch lengths was found.

Table 1 **Estimates of branching times (Myr ago) within the Catarrhini, using host and parasite phylogenies**

Branch point	SFV *pol*	COII	Fossil estimate*
Split Cercopithecoidea/Hominoidea	25–30	25–30	25–30
Cercopithecidae	22.9–24.4	23.6–27.7	–
Hominoidae(≡split Homonidae/Hylobatidae)	12–16	26.1	–
MRCA Hylobatidae	10.1–10.8	8.3–15.1	–
MRCA Ponginae	4.7–5.5	1.4–10.7	–
Split Homininae/Ponginae	n.a.†	18.5–23.5	~14
Split *Pan*/*Gorilla*	9.8–10.8	10.6–16.4‡	–
Split *Pan*/*Homo*	n.a.§	4.7–8.9	~5–6
MRCA *Pan*	5.9–6.6	1.2	–
Split *Cercocebus torquatus*/*M. sphinx*	–	1.4	–

Values for SFV and COII represent 95% confidence intervals; n.a., not available; MRCA, most recent common ancestor. The split of the Cercopithecoidea from the Hominoidea 25–30 Myr ago was used as a calibration point for the molecular dating of both SFV and COII sequences. Estimates and confidence intervals of the SFV and COII divergence times were determined on the maximum-likelihood tree topology by using the nonparametric rate smoothing algorithm implemented in the r8s program[21]. Values given without a range are the upper limit estimates.
*The fossil estimates for the Catarrhini are from refs 18 and 19.
†Hominidae and Ponginae do not form a monophyletic clade in the SFV tree.
‡Includes *Homo sapiens* sequence.
§A human-specific foamy virus has yet to be identified.

ago[20]. Thus, we propose FV to be the oldest known exogenous vertebrate RNA virus.

Under the assumption of co-speciation we were able to estimate the rate of nucleotide substitution in SFV. Although the presence of a strict molecular clock was weakly rejected for both the COII ($P = 0.005$) and SFV ($P = 0.004$) trees, the inferred substitution rates for the host and SFV genes were strikingly similar; assuming a calibration point of 25–30 Myr ago as the separation of the Hominoidea and Cercopithecoidea, the substitution rates for COII and SFV were estimated at $(1.16 \pm 0.35) \times 10^{-8}$ (MLE ± SE) and $(1.7 \pm 0.45) \times 10^{-8}$ substitutions per site per year, respectively. Similar substitution rates—$(1.03 \pm 0.42) \times 10^{-8}$ and $(1.83 \pm 0.93) \times 10^{-8}$, respectively—were obtained with the nonparametric rate smoothing program that does not assume a molecular clock[21]. SFV is therefore evolving so slowly that it approaches the rates recorded in protein-coding regions of mitochondrial DNA[22]. This substitution rate is the lowest ever reported for RNA viruses and is closer to those of DNA viruses (10^{-7} to 10^{-8} substitutions per site per year) and endogenous retroviruses ($(2.3–5.0) \times 10^{-9}$ substitutions per site per year) than to other exogenous RNA viruses such as HIV and influenza A virus (normally in the range 10^{-3} to 10^{-4} substitutions per site per year)[9,23–25].

The low substitution rates observed for SFV might be a function of their low rates of active replication, with most tissues latently infected[10]. FV expression is inhibited by negative regulation of an internal promoter unique to this group of retroviruses[26]. In addition, FV regulatory proteins have also been shown to induce the expression of cellular genes, including that encoding interferon, that are known to reduce viral expression[26]. Strong purifying selection and replication by means of a reverse transcriptase with a high fidelity will also reduce substitution rates. Whereas we found a greater number of synonymous (d_S) than non-synonymous (d_N) substitutions per site in the SFV *pol* sequences ($d_N/d_S = 0.161$), revealing the action of purifying selection, similar or greater levels of selective constraint have been observed in rapidly evolving RNA viruses[27] and in the primate COII sequences ($d_N/d_S = 0.069$). Although the fidelity of the SFV reverse transcriptase is unknown, our findings do not predict a high error rate per replication cycle as observed in HIV[25]. However, it is unlikely that the accuracy of SFV reverse transcription alone can fully explain the observed low substitution rate, and thus lower SFV expression in persistently infected hosts must also have a major role in producing the low rate of evolutionary change observed here.

Although most NHP species investigated so far harbour distinct and species-specific SFV lineages, evidence supporting the existence of a human-specific FV is not yet available. Instead, all FVs identified in humans are of simian origin in persons exposed to NHPs[10,11]. Despite humans having a common evolution with NHPs and being susceptible to SFV infection, it is not understood why humans are not endemically infected with a distinct FV. It is possible that in the past humans were infected with an FV that became extinct because of reduced transmissibility, a finding consistent with the difficulty of human-to-human spread of SFV from accidentally infected humans[10,11]. Alternatively, foci of endemically infected humans might exist but they have not yet been identified because of limited screening of small numbers of human populations[10].

Thus, we provide extensive evidence supporting the co-speciation of SFV and primates. The non-pathogenic nature of SFV in persistently infected natural hosts, the ubiquity of SFV in primates, the congruent SFV and primate phylogenies and the similarity in divergence times all support an ancient history of host–parasite co-speciation. □

Methods

Primate specimens and SFV serology

Fresh blood specimens were obtained opportunistically from captive and wild-born primates in accordance with the animal care and use committees at each institution. For PCR analysis, nucleic acids were prepared from peripheral blood lymphocytes (PBLs) as described previously[11]. All primates included in this study were determined as seropositive for SFV Gag antibodies in a combined antigen western blot assay as described[11]. The primate taxonomic nomenclature used here was as described[28] and were coded using the first letter of the genus and the first two letters of the species or subspecies names with their house names or codes within parentheses (Supplementary Information).

SFV isolation and propagation

SFV isolates from selected NHP species (Supplementary Information) were obtained by co-cultivation of NHP PBLs with Cf2Th cells as reported previously[11].

Amplification of SFV and mtDNA COII DNA sequences

A total of 32 new SFV and 50 new primate mtDNA COII sequences were determined in this study. Polymerase chain reaction (PCR) was performed with 1 μg of PBLs or PBL co-culture DNA in a generic nested amplification of a 465-base-pair SFV *pol* sequence by using methods described previously[11]; 556-base-pair COII sequences were amplified by using standard PCR conditions with a 50 °C annealing temperature, 200 ng of PBL DNA, and the generic primers PCO2F2 (5′-A(C/T)GC(C/T)CTI(C/T)(C/T)CI(C/T)(A/G)ACA CTCACAACAAA-3′) and PCO2R1 (5′-(G/A)AATAC(G/A)GG(T/C)CC(T/C)ATTTC (A/G)AAGATTTTTA-3′). The primers BCO2F2 (5′-ACGCCCTATCCTCAACACTCA CAACAAA-3′) and BCO2R1 (5′-GAACACAGGTCCTATTTCAAAGATTTTTA-3′) or ACO2F2 (5′-ACGCCCTTTTCCTAACACTCACAACAAA-3′) and ACO2R1 (5′-GAATACGGG(C/T)CC(C/T)ATTTC(A/G)AAGATTTTTA-3′) were used to amplify COII sequences from baboons or chimpanzees, respectively, using the same PCR conditions as above. COII sequences (1218 base pairs) were also amplified by reverse transcriptase PCR from mRNA obtained from the PBLs of selected primates (Supplementary Information) with the primers COII (5′-GCCACATCCCCTGTCATAGAAGA-3′) and APT6 (5′-GGTTTATAGAAAGTTGGGTGGTTGG-3′) and PCR conditions 94 °C for 1 min, 55 °C for 30 s, 72 °C for 1.5 min, for a total of 30 cycles. Standard precautions were always taken to avoid PCR contamination. PCR products were revealed on 1.5% agarose gels stained with ethidium bromide, purified with a Qiaquick PCR purification kit (Qiagen) and sequenced in both directions with a BigDye terminator cycle kit and automated sequencers (Applied Biosystems).

Sequence analysis

SFV and COII sequences were aligned by using the ClustalW program (http://www.cmbi.kun.nl/bioinf/CLUSTALW/). To minimize the effects of nuclear mtDNA pseudogenes on our analyses, only COII sequences with open reading frames were used. Identical COII sequences from the same species were omitted. Little substitution saturation was observed in the SFV and COII sequences ($P < 0.00001$), as determined with the DAMBE program (http://web.hku.hk/~xxia/software/software.htm), and they were therefore satisfactory for use in phylogenetic analyses. The best-fit phylogenetic model was determined with a likelihood ratio test and assumed the following nucleotide substitution rate pattern with maximum-likelihood estimated parameters: A to G and C to T = 12.3, A to C = 5.8, A to T and C to G = 3.1, G to T = 1.0; gamma-distributed rates (discrete approximation, eight categories) across sites with a maximum-likelihood estimate (MLE) of $\alpha = 0.37$, and unequal empirical nucleotide frequencies for the SFV alignment. This model was used to infer distance-based and maximum-likelihood trees. The best-fit substitution model for the COII sequences was HKY85 with gamma-distributed rates (transition/transversion = 12.1, $\alpha = 0.27$, MLE). This model was used to infer the COII maximum-likelihood tree. Neighbour-joining COII trees were inferred with LogDet/paralinear distances and the Moment Estimator technique enforcing the constraints of the HKY85 model. One thousand bootstrap replicates were used to assess the robustness of the final tree topology. All phylogenetic analyses were undertaken using the PAUP* package (http://www.paup.csit.fsu.edu/). To determine whether the SFV and COII sequences were behaving in a clock-like manner, the molecular-clock and variable-

rate phylogenetic trees were compared by using a likelihood ratio test.

Estimates and confidence intervals of the SFV divergence times were determined on the maximum-likelihood tree topology with the nonparametric rate smoothing algorithm implemented in the r8s program[21]. The branch lengths of the COII tree were re-estimated by enforcing a molecular clock with the PAUP* program. Confidence intervals for the COII divergence times were estimated with the r8s program by using the penalized likelihood algorithm[29] and 95% confidence intervals are given by 1.96σ. The split of the Cercopithecoidea from the Hominoidea 25–30 Myr ago was used as a calibration point for the molecular dating of both SFV and COII sequences[18,19]. The number of synonymous (d_S) and non-synonymous (d_N) substitutions per site were estimated with the program Diverge in the Genetic Computer Group Wisconsin Package (http://www.accelrys.com/products/gcg_wisconsin_package).

Reconciliation analysis and comparison of branch lengths of the SFV and COII trees were performed with the TreeMap (v1.0) program in accordance with the author's instructions (http://taxonomy.zoology.gla.ac.uk/rod/treemap.html)[30]. A single optimal reconstruction was found with the heuristic search option. The significance of the observed fit between the SFV and primate trees and branch lengths was determined by comparison with the distribution of the same measure of fit for 10,000 randomly generated trees or branch lengths by using the proportional-to-distinguishable model of the randomization test incorporated in TreeMap.

Received 7 September; accepted 22 December 2004; doi:10.1038/nature03341.

1. Hafner, M. S. *et al.* Disparate rates of molecular evolution in cospeciating hosts and parasites. *Science* **265,** 1087–1090 (1994).
2. Page, R. D. M. Temporal congruence and cladistic analysis of biogeography and cospeciation. *Syst. Zool.* **39,** 205–226 (1990).
3. Brooks, D. R. Analysis of host-parasite coevolution. *Int. J. Parasitol.* **17,** 291–297 (1987).
4. Charrel, R. N., De Micco, P. & de Lamballerie, X. Phylogenetic analysis of GB viruses A and C: evidence for cospeciation between virus isolates and their primate hosts. *J. Gen. Virol.* **80,** 2329–2335 (1999).
5. McGeoch, D. J., Dolan, A. & Ralph, A. C. Toward a comprehensive phylogeny for mammalian and avian herpesviruses. *J. Virol.* **74,** 10401–10406 (2000).
6. Charleston, M. A. & Robertson, D. L. Preferential host switching by primate lentiviruses can account for phylogenetic similarity with the primate phylogeny. *Syst. Biol.* **51,** 528–535 (2002).
7. Salemi, M. *et al.* Mosaic genomes of the six major primate lentivirus lineages revealed by phylogenetic analyses. *J. Virol.* **77,** 7202–7213 (2003).
8. Jackson, A. P. & Charleston, M. A. A cophylogenetic perspective of RNA-virus evolution. *Mol. Biol. Evol.* **21,** 45–57 (2004).
9. Holmes, E. C. Molecular clocks and the puzzle of RNA virus origins. *J. Virol.* **77,** 3893–3897 (2003).
10. Meiering, C. D. & Linial, M. L. Historical perspective of foamy virus epidemiology and infection. *Clin. Microbiol. Rev.* **14,** 165–176 (2001).
11. Hussain, A. I. *et al.* Screening for simian foamy virus infection by using a combined antigen Western blot assay: evidence for a wide distribution among Old World primates and identification of four new divergent viruses. *Virology* **309,** 248–257 (2003).
12. Disotell, T. R., Honeycutt, R. L. & Ruvolo, M. Mitochondrial DNA phylogeny of the Old-World monkey tribe Papionini. *Mol. Biol. Evol.* **9,** 1–13 (1992).
13. Ruvolo, M., Disotell, T. R., Allard, M. W., Brown, W. M. & Honeycutt, R. L. Resolution of the African hominoid trichotomy by use of a mitochondrial gene sequence. *Proc. Natl Acad. Sci. USA* **88,** 1570–1574 (1991).
14. Adkins, R. M. & Honeycutt, R. L. Evolution of the primate cytochrome C oxidase subunit II gene. *J. Mol. Evol.* **38,** 215–231 (1994).
15. van der Kuyl, A. C., Kuiken, C. L., Dekker, J. T. & Goudsmit, J. Phylogeny of African monkeys based upon mitochondrial 12S rRNA sequences. *J. Mol. Evol.* **40,** 173–180 (1995).
16. Page, S. L., Chiu, C. H. & Goodman, M. Molecular phylogeny of Old World monkeys (*Cercopithecidae*) as inferred from gamma-globin DNA sequences. *Mol. Phylogenet. Evol.* **13,** 348–359 (1999).
17. Harris, E. E. & Disotell, T. R. Nuclear gene trees and the phylogenetic relationships of the mangabeys (Primates: Papionini). *Mol. Biol. Evol.* **15,** 892–900 (1998).
18. Goodman, M. *et al.* Toward a phylogenetic classification of Primates based on DNA evidence complemented by fossil evidence. *Mol. Phylogenet. Evol.* **9,** 585–598 (1998).
19. Page, S. L. & Goodman, M. Catarrhine phylogeny: noncoding DNA evidence for a diphyletic origin of the mangabeys and for a human-chimpanzee clade. *Mol. Phylogenet. Evol.* **18,** 14–25 (2001).
20. Murphy, W. J. *et al.* Resolution of the early placental mammal radiation using Bayesian phylogenetics. *Science* **294,** 2348–2351 (2001).
21. Sanderson, M. J. r8s: inferring absolute rates of molecular evolution and divergence times in the absence of a molecular clock. *Bioinformatics* **19,** 301–302 (2003).
22. Ruvolo, M. *et al.* Mitochondrial COII sequences and modern human origins. *Mol. Biol. Evol.* **10,** 1115–1135 (1993).
23. Shadan, F. F. & Villarreal, L. P. Coevolution of persistently infecting small DNA viruses and their hosts linked to host-interactive regulatory domains. *Proc. Natl Acad. Sci. USA* **90,** 4117–4121 (1993).
24. Johnson, W. E. & Coffin, J. M. Constructing primate phylogenies from ancient retrovirus sequences. *Proc. Natl Acad. Sci. USA* **96,** 10254–10260 (1999).
25. Suzuki, Y., Yamaguchi-Kabata, Y. & Gojobori, T. Nucleotide substitution rates of HIV-1. *AIDS Rev.* **2,** 39–47 (2000).
26. Löchelt, M. Foamy virus transactivation and gene expression. *Curr. Top. Microbiol. Immunol.* **277,** 27–61 (2003).
27. Woelk, C. H. & Holmes, E. C. Reduced positive selection in vector-borne RNA viruses. *Mol. Biol. Evol.* **19,** 2333–2336 (2002).
28. Groves, C. *Primate Taxonomy* (Smithsonian Institution Press, Washington DC, 2001).
29. Sanderson, M. J. Estimate absolute rates of molecular evolution and divergence times: a penalized likelihood approach. *Mol. Biol. Evol.* **19,** 101–109 (2002).
30. Page, R. D. M. Parallel phylogenies: reconstructing the history of host-parasite assemblages. *Cladistics* **10,** 155–173 (1994).

Supplementary Information accompanies the paper on **www.nature.com/nature.**

Acknowledgements We thank the veterinary staff at all zoological gardens and primate centres who kindly provided blood specimens from the primates living at their institutions; R. Heberle and P. Johnston for the SFV-infected baboon and orangutan isolates; A. Hussain and A. Wright for expert technical assistance; and A. Vandamme, C. Coulibaly, M. Peeters, F. Bibollet-Ruche, V. Hirsch, J. Allan, T. Butler and H. McClure for providing additional primate samples for this study.

Competing interests statement The authors declare that they have no competing financial interests.

Correspondence and requests for materials should be addressed to W.M.S. (bis3@cdc.gov). The GenBank accession numbers for the 32 new SFV *pol* and 50 new primate mtDNA COII sequences are AY686124–AY686148 and AY686150–AY686206.

Genetic relatedness predicts South African migrant workers' remittances to their families

S. Bowles[1] & D. Posel[2]

[1]*Santa Fe Institute, 1399 Hyde Park Rd, Santa Fe, New Mexico 87501, USA; and Università degli Studi di Siena, Piazza San Francesco, Siena 53100, Italy*
[2]*University of KwaZulu-Natal, King George V Avenue, Durban 4001, South Africa*

Inclusive fitness models[1,2] predict many commonly observed behaviours: among humans, studies of within-household violence[3], the allocation of food[4,5] and child care[6] find that people favour those to whom they are more closely related. In some cases however, kin-altruism effects appear to be modest[7–9]. Do individuals favour kin to the extent that kin-altruism models predict? Data on remittances sent by South African migrant workers to their rural households of origin allow an explicit test, to our knowledge the first of its kind for humans. Using estimates of the fitness benefits and costs associated with the remittance, the genetic relatedness of the migrant to the beneficiaries of the transfer, and their age- and sex-specific reproductive values, we estimate the level of remittance that maximizes the migrant worker's inclusive fitness. This is a much better predictor of observed remittances than is average relatedness, even when we take account (by means of a multiple regression) of covarying influences on the level of remittance. But the effect is modest: less than a third of the observed level of remittances can be explained by our kin-altruism model.

Migrants' remittances provide a rare window into the allocation of resources within a household, as intra-household transfers are typically not measured in surveys. The large and genetically heterogeneous nature of rural African households makes migrants and their households of origin an ideal database. The data for our study come from a nationally representative survey in 1993 of approximately 9,000 households[10].

We have complete data on the income, remittances received, land ownership and composition of the household of origin, and on each migrant worker's age and schooling for 539 black male migrants. Virtually all migrants in the sample sent remittances in the year preceding the survey in 1993, and on average they sent almost half of their urban wage. Figure 1 shows the distribution of average relatedness of the migrant to the household of origin. (Consanguineous marriages are exceptionally rare in South Africa[11], so we assume that the migrant and his wife are unrelated.)

Hamilton's rule states that conferring a fitness benefit (b) by helping another at a cost of (c) to oneself will be selected for if $rb > c$, where r is the genetic relatedness of the donor to the beneficiary. Here we consider a case in which the choice is not